

Multipath Parameter Estimation from OFDM Signals in Mobile Channels

Nick Letzepis, *Member, IEEE*, Alex Grant, *Senior Member, IEEE*,
Paul Alexander *Member, IEEE*, David Haley, *Member, IEEE*

Abstract

We study multipath parameter estimation from orthogonal frequency division multiplex signals transmitted over doubly dispersive mobile radio channels. We are interested in cases where the transmission is long enough to suffer time selectivity, but short enough such that the time variation can be accurately modeled as depending only on per-tap linear phase variations due to Doppler effects. We therefore concentrate on the estimation of the complex gain, delay and Doppler offset of each tap of the multipath channel impulse response. We show that the frequency domain channel coefficients for an entire packet can be expressed as the superimposition of two-dimensional complex sinusoids. The maximum likelihood estimate requires solution of a multidimensional non-linear least squares problem, which is computationally infeasible in practice. We therefore propose a low complexity suboptimal solution based on iterative successive and parallel cancellation. First, initial delay/Doppler estimates are obtained via successive cancellation. These estimates are then refined using an iterative parallel cancellation procedure. We demonstrate via Monte Carlo simulations that the root mean squared error statistics of our estimator are very close to the Cramer-Rao lower bound of a single two-dimensional sinusoid in Gaussian noise.

I. INTRODUCTION

In wireless communications, reflection and diffraction of the transmitted radio signal results in the superimposition of multiple complex-scaled and delayed copies of the signal at the receiver.

N. Letzepis and A. Grant are with the Institute for Telecommunications Research, University of South Australia, e-mail: nick.letzepis@ieee.org, alex.grant@unisa.edu.au. P. Alexander and D. Haley are with Cohda Wireless Pty. Ltd., e-mail: {paul.alexander,david.haley}@cohdawireless.com.au.

This work was supported by Cohda Wireless Pty. Ltd. and the Australian Research Council under grant LP0775036.

This type of channel is commonly referred to as a *multipath channel*. In some instances, the multiple copies add constructively, and in others destructively resulting in *multipath fading*. When the coherence bandwidth of the channel is smaller than the bandwidth of the radio signal then the fading is termed *frequency selective* [1]. We assume the reader is familiar with standard wide-sense stationary uncorrelated scattering models, for an overview see e.g. [2].

Orthogonal frequency division multiplexing (OFDM) is a transmission strategy specifically designed to combat frequency selective channels with relatively low receiver complexity [3–5]. In OFDM, the signal bandwidth is divided into several non-overlapping (hence orthogonal) narrowband subcarriers where the width of each subchannel is chosen such that it is approximately frequency non-selective. Thus only a single tap equaliser per subchannel is required to compensate for the multipath fading. Together with the use of the fast Fourier transform (FFT), this results in a low complexity way to handle frequency-selective channels. As such, OFDM is now the basis of many current and emerging wireless communications standards, see [6, 7] for an overview. Many of these standards are targeted for outdoor mobile applications, e.g. 802.11p [8]. Mobility causes the multipath channel (and hence frequency selectivity) to change with time. If the mobility is fast enough compared to the symbol rate, then the channel impulse response may vary significantly within an OFDM packet. Extensive field trials have shown that this is indeed the case for the transmission of 802.11 OFDM signals in vehicular environments [9]. Time-varying multipath channels such as these are commonly termed *doubly-dispersive* [10–12].

In general, a realization of a doubly selective multipath channel time-varying impulse response can be modeled in continuous time as

$$c(t, \tau) = \sum_{p=1}^P a_p(t) \delta(\tau - \tau_p)$$

where $c(t, \tau)$ is the response at delay τ to an impulse at time t , where $\delta(\tau)$ denotes the Dirac-delta function. The $a_p(t)$ are the time-varying complex amplitude (magnitude and phase) of tap p , with delay τ_p . The number of resolvable multipath components is P . The $a_p(t)$ may aggregate many more unresolvable multipath components, typically resulting in Ricean or Rayleigh statistics for these parameters.

Note that for sufficiently short time durations, mobility-induced Doppler shifts manifest as linear variations of the phase of $a_p(t)$ with time. In this paper, we consider the special case

where the OFDM packet duration is short enough such that we can model the channel as

$$c(t, \tau) = \sum_{p=1}^P a_p e^{-j2\pi\nu_p t} \delta(\tau - \tau_p), \quad (1)$$

where a_p , τ_p and ν_p respectively denote the complex gain, delay and Doppler frequency (relative to the nominal carrier frequency) of tap p . These parameters are all assumed to be *constant* over the duration of an OFDM packet. In a physical sense, this implies that changes in the relative distance and velocity between the transmitter, receiver and scatterers are negligible over the duration of an OFDM packet. This model is consistent with the geometric-stochastic model presented in [13] for short observation windows, and has been validated experimentally in [9].

In this paper, we concentrate on joint estimation of a_p , τ_p and ν_p of the multipath components assuming perfect knowledge of the transmitted OFDM symbols. This is a practical assumption, e.g. a transmitted training/pilot signal, or the receiver is able to decode the signal without error (via a forward error correction code). Estimation of these parameters is useful in a number of areas: channel sounding and characterisation; channel prediction; reducing channel state information for feedback in adaptive communications; and radar. Estimation of these parameters in the OFDM setting has been studied previously by a number of researchers from both the communications and radar fields. Channel estimation via an approximate maximum likelihood parameter search algorithm was proposed by Thomas *et al.* [14]. Their iterative algorithm was based on an approximation of the maximum likelihood function, where the multipath gain values are substituted with their least-squares estimates. In the radar community, estimation of delay/Doppler is vital for determination of target range and velocity. Berger *et al.* [15] studied the problem of extracting the target range/velocity information from the OFDM signal in a passive multi-static radar system [16] using digital audio/video broadcasted signals as illuminators of opportunity. They set up the problem as a sparse estimation problem to use recent results from compressed sensing [17]. In particular, they employ the orthogonal matching pursuit algorithm [18, 19], which is an iterative algorithm that successively removes previously estimated multipath components from the received signal to estimate new components. Note that Tauböck *et al.* [20, 21] also consider compressed sensing to estimate the OFDM channel coefficients. However, their interest is not in the estimation of delays/Doppler, but in the frequency/time channel coefficients.

In this paper we begin with a continuous-time model of the transmitted OFDM signal and

derive the received matched filtered signal from first principles. Assuming the delay-spread of the channel does not exceed the cyclic-prefix and the pass-band of the receive/transmit filters exceed the signal bandwidth (with negligible pass-band ripple), we show that the resulting frequency domain channel coefficients can be represented as the superimposition of two-dimensional (2-D) complex sinusoids, where each 2-D frequency is proportional to the delay and Doppler of each multipath component. Similar observations have been made by Wong and Evans [22, 23] although without detailed justification. Under a similar setting they consider estimation using only OFDM pilot symbols and propose channel prediction algorithms based on the estimation of channel parameters via a rotational invariance technique. Using this method, they reformulate the problem as a one-dimensional estimation problem.

Parameter estimation of 2-D sinusoids in a general setting has been studied extensively many years prior to the work of Wong and Evans [22, 23]. Estimation methods and the Cramer-Rao-Lower-Bound (CRLB) for the single 2-D sinusoid case was investigated by Chien [24]. Kay and Nekovei [25] proposed a low complexity estimator that operates on the phase of the noisy 2-D sample data. For the estimation of the superposition of multiple 2-D sinusoids: Bresler and Macovski employ a 2-D version of Prony's method [26]; Rao *et al.* [27] use a similar polynomial rooting approach; and recently Kliger and Francos [28] consider maximum-likelihood estimation with a maximum a-posteriori (MAP) model order selection rule for the case where the number of sinusoids is unknown.

In this paper we concentrate purely on the estimation of the complex amplitude, delay and Doppler of each multipath tap, assuming the number of taps is known. Our results can be straightforwardly extended to the case where the number of taps is unknown using well-known *model-order selection* methods [29]. The maximum-likelihood approach requires the solution to a multi-dimensional nonlinear least-squares estimation problem [30] and hence has complexity that is prohibitive in practice [26–28]. We propose a low-complexity algorithm based on a two-stage process: first, an initial estimation; followed by a refinement procedure. In the same spirit as [14, 15, 28] the initial estimation algorithm is based on successive cancellation, whereby multipath components are subtracted from the original signal after they are detected. In each iteration, the delay/Doppler is estimated using periodogram search [24, 25] via a 2-D bisection algorithm. The multipath complex amplitudes are then obtained via standard linear least-square estimation [31]. Moreover, we show that this secondary problem can be written in terms of

the *ambiguity function* [32]. Once initial estimates have been obtained, we then propose an iterative refinement algorithm based on parallel cancellation. Each iteration of the refinement involves subtracting all multipath components from the received signal except the component of interest, which is re-estimated using the 2-D bisection algorithm. This refinement process yields significant improvements over the standard successive cancellation approach. We show via Monte-Carlo simulations that this refinement algorithm achieves performance very close to the CRLB for single 2-D sinusoid estimation.

The remainder of our paper is organised as follows. In Section II we state the system model and derive from first principles the received match filtered frequency domain OFDM symbols. In Section III we derive the transmit signal ambiguity function. Then in Section IV we present our proposed estimation algorithm and enhanced refinement process. Simulation results are presented in Section V. Finally, concluding remarks are given in Section VI.

II. SYSTEM MODEL

Consider a K subcarrier OFDM system, where packets of length L OFDM symbols are transmitted. Let $\mathbf{X} \in \mathbb{C}^{L \times K}$ denote a packet of complex OFDM symbols. Thus $X_{l,k}$, the l, k th element of \mathbf{X} , denotes the l th symbol transmitted on subcarrier k , for $l = 1, \dots, L$ and $k = 1, \dots, K$. In practical OFDM systems, a certain number *null* subcarriers are employed to simplify receiver design [5]. To incorporate this feature, we let \mathcal{K} denote the set of null subcarrier indices. Thus, $X_{l,k} = 0$ for all $k \in \mathcal{K}$ and $l = 1, \dots, L$. For all other subcarriers, i.e. $k \notin \mathcal{K}$, we assume $X_{k,l} \in \mathcal{X}$, where $\mathcal{X} \subset \mathbb{C}$ is an arbitrary complex constellation. These symbols are drawn randomly, independently and uniformly from \mathcal{X} , which is normalised to have unit average energy. Thus $\mathbb{E}[|X_{l,k}|^2] = 1$ for $k \notin \mathcal{K}$ and $\mathbb{E}[X_{l,k}X_{n,m}^*] = 0$ for any $n \neq l$ or $m \neq k$. The receiver is assumed to have complete knowledge of the transmitted symbols $X_{l,k}$, e.g. a pilot/training signal, or from the feedback of error-free decoder decisions.

Let $x(t) = \sum_{l=1}^L x_l(t)$ denote the complex baseband continuous-time transmitted OFDM signal, where

$$x_l(t) = \frac{1}{\sqrt{KL}} \sum_{k=1}^K X_{l,k} e^{j2\pi(k-1-\lfloor K/2 \rfloor)(t-T_{\text{cp}})/T} w(t - (l-1)T_d), \quad (2)$$

is the l th OFDM symbol, T_d is the OFDM symbol duration (seconds), $1/T$ is the subcarrier spacing (Hz), $T_{\text{cp}} = T_d - T$ is the cyclic prefix duration (seconds), and $w(t)$ is a windowing

function such that

$$w(t) = \begin{cases} \tilde{w}(t) & 0 \leq t \leq T_d \\ 0 & \text{otherwise,} \end{cases} \quad (3)$$

and $\int_0^{T_d} |w(t)|^2 dt = 1$. A simple choice of windowing function is $\tilde{w}(t) = 1/\sqrt{T_d}$. Note that the assumption $w(t) = 0$ for $t \notin (0, T_d)$ is not necessarily required, but we assume this for simplicity. In practice, (2) is implemented in the discrete time domain via the inverse discrete Fourier transform (IDFT) [5].

We assume transmit and receive filter impulse responses $g_T(t)$ and $g_R(t)$ respectively, and let $g(t) \triangleq \int_{-\infty}^{\infty} g_T(u)g_R(t-u) du$ denote the combined transmit/receive filter response. Thus, using (1), we write the overall channel response as

$$h(t, \tau) = \int_{-\infty}^{\infty} g(u)c(t, \tau - u) du = \sum_{p=1}^P a_p e^{-j2\pi\nu_p t} g(\tau - \tau_p). \quad (4)$$

Application of the overall channel response (4) to (2) plus additive Gaussian white noise (AWGN) yields the received continuous-time baseband signal,

$$y(t) = \sum_{\nu} \int_{-\infty}^{\infty} x_{\nu}(t - \tau)h(t, \tau) d\tau + z(t), \quad (5)$$

where $z(t) = \int_{-\infty}^{\infty} \tilde{z}(t-u)g_R(u) du$, and $\tilde{z}(t)$ is an additive white Gaussian noise (AWGN) process. Assuming perfect OFDM symbol synchronism, the receiver discards the cyclic prefix and performs the matched filter to the transmitted sinusoids, i.e.

$$Y_{l,k} = \frac{1}{\sqrt{KL}} \int_{T_{cp}+(l-1)T_d}^{lT_d} y(t)w^*(t - (l-1)T_d)e^{-j2\pi(k-1-\lfloor K/2 \rfloor)(t-T_{cp})/T} dt, \quad (6)$$

for $k = 1, \dots, K$ and $l = 1, \dots, L$. Note that in practice, $Y_{l,k}$ is obtained via the discrete Fourier transform (DFT) [5]. We assume the pass-band of filters g_T and g_R exceed the signal bandwidth. In addition, we assume $\max_p \tau_p < T_{cp}$ and $\max_p |\nu_p| < 1/T$, so that inter-symbol interference (ISI) and inter-carrier interference (ICI) can be considered negligible. Under these assumptions, in Appendix I we show that the matched filtered output (6) can be written in matrix form

$$\mathbf{Y} = \mathbf{H} \odot \mathbf{X} + \mathbf{Z}, \quad (7)$$

where \odot denotes the element-wise (Hadamard) product, $\mathbf{Y} \in \mathbb{C}^{L \times K}$ is the received matrix of filtered noisy OFDM symbols, $\mathbf{Z} \in \mathbb{C}^{L \times K}$ is a matrix of independent identically distributed

(i.i.d.) zero mean complex Gaussian random variables with variance σ^2 , and $\mathbf{H} \in \mathbb{C}^{L \times K}$ are the frequency domain channel coefficients,

$$H_{l,k} = \sum_{p=1}^P a_p e^{-j2\pi\nu_p T_d(l-1)} e^{-j2\pi(k-1-\lfloor K/2 \rfloor)\tau_p/T}. \quad (8)$$

In relation to (7), we define the signal-to-noise ratio (SNR) as $\text{snr} \triangleq \mathbb{E}[\|\mathbf{X}\|^2]/(L\sigma^2) = (K - |\mathcal{K}|)/\sigma^2$, where $\|\cdot\|$ denotes the Frobenius norm [33].

From inspection of (8), we see that it is simply the superimposition of 2-dimensional (2-D) complex exponential signals. We may also express \mathbf{H} as the matrix product

$$\mathbf{H} = \mathbf{\Psi}(\boldsymbol{\nu}) \text{diag}(\mathbf{a}) \mathbf{\Phi}^\dagger(\boldsymbol{\tau}), \quad (9)$$

where $\text{diag}(\mathbf{a})$ denotes a $P \times P$ diagonal matrix with diagonal entries $\mathbf{a} = (a_1, \dots, a_P)$, and

$$\Psi_{l,p}(\boldsymbol{\nu}) = \psi_l(\nu_p) \triangleq e^{-j2\pi(l-1)\nu_p T_d} \quad (10)$$

$$\Phi_{k,p}(\boldsymbol{\tau}) = \phi_k(\tau_p) \triangleq e^{j2\pi(k-1-\lfloor K/2 \rfloor)\tau_p/T}, \quad (11)$$

for $p = 1, \dots, P$, $l = 1, \dots, L$ and $k = 1, \dots, K$. As we shall see later, the separation of the parameters in this matrix form will simplify the development of our estimation algorithms.

In the analysis that is to follow, we will make use of the vectorised version of (7). Let $\mathbf{y} = \text{vec}(\mathbf{Y}) = (Y_{1,1}, \dots, Y_{L,1}, Y_{1,2}, \dots, Y_{L,2}, \dots, Y_{1,K}, \dots, Y_{L,K})'$, and $\mathbf{z} = \text{vec}(\mathbf{Z})$ then

$$\mathbf{y} = \mathbf{\Omega}(\boldsymbol{\tau}, \boldsymbol{\nu}, \mathbf{X}) \mathbf{a} + \mathbf{z}. \quad (12)$$

where the $KL \times P$ matrix $\mathbf{\Omega}$ is a function of $\boldsymbol{\tau}$, $\boldsymbol{\nu}$, and \mathbf{X} as follows,

$$\mathbf{\Omega}(\boldsymbol{\tau}, \boldsymbol{\nu}, \mathbf{X}) = \begin{pmatrix} X_{1,1}\psi_1(\nu_1)\phi_1^*(\tau_1) & X_{1,1}\psi_1(\nu_2)\phi_1^*(\tau_2) & \dots & X_{1,1}\psi_1(\nu_P)\phi_1^*(\tau_P) \\ \vdots & \vdots & & \vdots \\ X_{L,1}\psi_L(\nu_1)\phi_1^*(\tau_1) & X_{L,1}\psi_1(\nu_2)\phi_1^*(\tau_2) & \dots & X_{L,1}\psi_L(\nu_P)\phi_1^*(\tau_P) \\ X_{1,2}\psi_1(\nu_1)\phi_2^*(\tau_1) & X_{1,2}\psi_1(\nu_2)\phi_2^*(\tau_2) & \dots & X_{1,2}\psi_1(\nu_P)\phi_2^*(\tau_P) \\ \vdots & \vdots & & \vdots \\ X_{L,2}\psi_L(\nu_1)\phi_2^*(\tau_1) & X_{L,2}\psi_1(\nu_2)\phi_2^*(\tau_2) & \dots & X_{L,2}\psi_L(\nu_P)\phi_2^*(\tau_P) \\ \vdots & \vdots & & \vdots \\ X_{1,K}\psi_1(\nu_1)\phi_K^*(\tau_1) & X_{1,K}\psi_1(\nu_2)\phi_K^*(\tau_2) & \dots & X_{1,K}\psi_1(\nu_P)\phi_K^*(\tau_P) \\ \vdots & \vdots & & \vdots \\ X_{L,K}\psi_L(\nu_1)\phi_K^*(\tau_1) & X_{L,K}\psi_L(\nu_2)\phi_K^*(\tau_2) & \dots & X_{L,K}\psi_L(\nu_P)\phi_K^*(\tau_P) \end{pmatrix}, \quad (13)$$

where $(\cdot)^*$ denotes the complex conjugate.

III. AMBIGUITY FUNCTION

The ambiguity function of the transmitted signal $x(t)$ is defined as the inner product of the signal with a delayed, frequency shifted version of itself [32]

$$A_x(\tau, \nu) = \int_{-\infty}^{\infty} x(t)x^*(t - \tau)e^{-j2\pi\nu t} dt. \quad (14)$$

In the context of OFDM communications the ambiguity function has been used often as a tool for pulse design and optimisation [10, 11]. In radar systems, the ambiguity function plays an important role in determining target range and velocity resolution [32]. In this section we derive the ambiguity function of the transmitted OFDM signal and highlight important characteristics that will affect the delay/Doppler estimation problem. Moreover, as we shall see later, parts of the estimation problem can be written succinctly in terms of the ambiguity function. In this direction, substitution of (2) into (14) yields the following result.

Theorem 1 (OFDM Ambiguity Function). *For a general windowing function $w(t)$, let $A_w(\nu, \tau)$ denote its ambiguity function. The ambiguity function of the OFDM signal (2) is,*

$$A_x(\tau, \nu) = \frac{e^{-j\pi K\tau/T}}{KL} \sum_{l,k,l',k'} X_{l,k} X_{l',k'}^* e^{-j2\pi(k-k')T_{cp}/T} e^{j2\pi(k'-1)\tau/T} e^{-j2\pi T_d(l-1)(\nu - \frac{k-k'}{T})} \times A_w(\tau + (l' - l)T_d, \nu + (k' - k)/T). \quad (15)$$

Due to the quadruple summation, numerical evaluation of (15) is computationally demanding. However, under some common practical design assumptions we can make further simplifications. Firstly, the windowing function is usually designed such that $A_w(\tau, \nu) \approx 0$ for $|\tau| > T_d$. Window functions of the form (3) will have this property. Thus the terms when $l' \neq l$ in the summation of (15) are approximately zero. Secondly, although $A_w(\tau, \nu)$ cannot be considered negligible for $|\nu| > (k' - k)/T$, since $X_{l,k}$ are i.i.d. with zero mean and unit variance by assumption (except for the null subcarriers, which have zero power), the summation of terms over $k \neq k'$ will approach zero for large K and/or L . In addition, since we are primarily concerned with delay and Doppler in the region $0 \leq \tau \leq T_{cp}$ and $|\nu| \ll 1/T$, where there is negligible variation in $A_w(\tau, \nu)$, we may assume $A_w(\tau, \nu) \approx A_w(0, 0)$, which only introduces a constant phase offset, since $|A_w(0, 0)|^2 = 1$. Hence we ignore the complex scaling affects of $A_w(\tau, \nu)$ and

approximate (15) as

$$A_x(\tau, \nu) \approx \tilde{A}_x(\tau, \nu) \triangleq \frac{1}{KL} \sum_{k,l} |X_{l,k}|^2 e^{-j2\pi(l-1)\nu T_d} e^{j2\pi(k-1-\lfloor K/2 \rfloor)\tau/T}. \quad (16)$$

In light of (15), note that (16) is also the ambiguity function when ISI and ICI can be considered negligible.

For phase shift keying (PSK) modulation, $|X_{l,k}| = 1$ with no null subcarriers, i.e. $\mathcal{K} = \emptyset$, then using the geometric summation formula, the ambiguity function (16) further simplifies to

$$\tilde{A}_x(\tau, \nu) \approx e^{-j\pi K\tau/T} \operatorname{sinc}\left(\pi K \frac{\tau}{T}\right) \operatorname{sinc}(\pi L\nu T_d), \quad (17)$$

where $\operatorname{sinc}(x) = \sin(x)/x$. Note that (17) is also equal to the expectation of (15) over the transmitted symbols $X_{l,k}$, i.e. it is the expected ambiguity function, $\mathbb{E}[A_x(\tau, \nu)]$, for an arbitrary signal constellation \mathcal{X} with zero mean and unit variance. In many OFDM standards, subcarrier $k = \lfloor K/2 \rfloor + 1$ is a null subcarrier. For these special cases (17) becomes,

$$\tilde{A}_x(\tau, \nu) \approx e^{-j\pi K\tau/T} \cos[\pi(K/2 + 1)(\tau/T)] \operatorname{sinc}(\pi\tau K/(2T)) \operatorname{sinc}(\pi\nu T_d L) \quad (18)$$

From the above expressions (17) and (18), we see that the sinc terms introduce sidelobes in the ambiguity function. Interestingly, the sidelobes are de-coupled in time and frequency. As an example, the ambiguity function of the 802.11a standard [34, 35] is plotted in Fig. 1, i.e. $K = 53$ subcarriers, with a null subcarrier at $k = \lfloor K/2 \rfloor + 1$, $T_d = 8 \mu\text{sec}$ and $T = 6.4 \mu\text{sec}$. From Fig. 1, as predicted by (18) we see that increasing L improves the Doppler resolution, but not the delay resolution, which is dependent only on K and the subcarrier spacing ($1/T$).

IV. MULTIPATH PARAMETER ESTIMATION

Our primary objective is to estimate $\mathbf{a} = (a_1, \dots, a_P)$, $\boldsymbol{\tau} = (\tau_1, \dots, \tau_P)$ and $\boldsymbol{\nu} = (\nu_1, \dots, \nu_P)$ in (1) from the received noisy symbols \mathbf{Y} (6) given perfect knowledge of \mathbf{X} . In this section, without loss of generality, for brevity of notation, we assume the OFDM system has no null subcarriers, i.e. $\mathcal{K} = \emptyset$. Using (12), the maximum likelihood (ML) approach is to solve the following

$$(\hat{\mathbf{a}}, \hat{\boldsymbol{\tau}}, \hat{\boldsymbol{\nu}}) = \arg \min_{\mathbf{a}, \boldsymbol{\tau}, \boldsymbol{\nu}} \|\mathbf{y} - \boldsymbol{\Omega}(\boldsymbol{\tau}, \boldsymbol{\nu}, \mathbf{X})\mathbf{a}\|^2, \quad (19)$$

which is a non-linear least squares minimisation problem. The computational complexity can be reduced by replacing \mathbf{a} with its least squares estimate. That is, for a given $\boldsymbol{\tau}$ and $\boldsymbol{\nu}$ the ML

estimate of \mathbf{a} is a linear least squares minimisation problem, which has solution [31]

$$\hat{\mathbf{a}} = (\mathbf{\Omega}^\dagger \mathbf{\Omega})^{-1} \mathbf{\Omega}^\dagger \mathbf{y}, \quad (20)$$

where we have dropped the dependence of \mathbf{X} , $\boldsymbol{\tau}$ and $\boldsymbol{\nu}$ for brevity of notation. Hence substituting (20) for \mathbf{a} in (19) results in the reduced problem

$$(\hat{\boldsymbol{\tau}}, \hat{\boldsymbol{\nu}}) = \arg \max_{\boldsymbol{\tau}, \boldsymbol{\nu}} \mathbf{y}^\dagger \mathbf{\Omega} (\mathbf{\Omega}^\dagger \mathbf{\Omega})^{-1} \mathbf{\Omega}^\dagger \mathbf{y}. \quad (21)$$

It is known that problems (21) and (19) are equivalent, i.e. (21) followed by (20) is also the ML solution [26, 36]. Unfortunately, (21) is in general multimodal, rendering the multidimensional search for a global extremum computationally prohibitive.

Before we begin our reduced complexity suboptimal solution, let us first make some interesting observations about (21). Let $\mathbf{R} = \mathbf{\Omega}^\dagger \mathbf{\Omega}$ and $\mathbf{w} = \mathbf{\Omega}^\dagger \mathbf{y}$. From (13), it is straightforward to show,

$$R_{ij} = KL \tilde{A}_x(\tau_i - \tau_j, \nu_j - \nu_i) \quad (22)$$

$$w_i = \boldsymbol{\psi}^\dagger(\nu_i) (\mathbf{Y} \odot \mathbf{X}^*) \boldsymbol{\phi}(\tau_i), \quad (23)$$

for $i, j = 1, \dots, P$, where $\boldsymbol{\psi}(\nu_i)$ and $\boldsymbol{\phi}(\tau_i)$ denote column i of the matrices $\boldsymbol{\Psi}$ and $\boldsymbol{\Phi}$ respectively, and \mathbf{A}^* denotes the element-wise conjugate of the matrix \mathbf{A} . Thus, rather than performing computation of $\mathbf{R} = \mathbf{\Omega}^\dagger \mathbf{\Omega}$ (requiring on the order of $PKL(KL+1)/2$ complex multiply-accumulate operations) using standard matrix operations, to reduce complexity, \mathbf{R} can be evaluated using the ambiguity function via a look-up table. Moreover, for the special case of PSK modulation, (17) implies we only need the evaluation of a $\text{sinc}(x)$ function.

For the special case of $P = 1$, the ML solution (21) becomes

$$(\hat{\tau}_1, \hat{\nu}_1) = \arg \max_{\tau, \nu} \left| \boldsymbol{\psi}^\dagger(\nu_1) (\mathbf{Y} \odot \mathbf{X}^*) \boldsymbol{\phi}(\tau_1) \right|^2, \quad (24)$$

after which the corresponding complex gain ML estimates can be determined using (20),

$$\hat{a}_1 = \frac{1}{KL} \boldsymbol{\psi}^\dagger(\hat{\nu}_1) (\mathbf{Y} \odot \mathbf{X}^*) \boldsymbol{\phi}(\hat{\tau}_1). \quad (25)$$

We see that the solution to (21) corresponds to the maximum absolute value of the 2-D periodogram [37]. Moreover, the CRLB for the estimation of a single tap multipath channel can be written as [24]

$$\text{var}[\hat{\nu}_1 T_d] \geq \frac{1}{4\pi^2} \frac{6}{KL(L^2 - 1)} \frac{\sigma^2}{|a_1|^2}, \quad \text{var}[\hat{\tau}_1/T] \geq \frac{1}{4\pi^2} \frac{6}{KL(K^2 - 1)} \frac{\sigma^2}{|a_1|^2}. \quad (26)$$

Note that Kay and Nekovei [25] proposed a low complexity weighted phase averager estimator as an alternative to solving (24).

If we were to use (24) when multiple taps are present ($P > 1$), then

$$\boldsymbol{\psi}^\dagger(\nu) (\mathbf{Y} \odot \mathbf{X}^*) \boldsymbol{\phi}(\tau) = KL \sum_p a_p \tilde{A}_x(\nu_p - \nu, \tau - \tau_p) + \boldsymbol{\psi}^\dagger(\nu) [\mathbf{Z} \odot \mathbf{X}^*] \boldsymbol{\phi}(\tau),$$

which is the superimposition of complex scaled, delay and frequency shifted ambiguity functions, plus an additive Gaussian noise term. We see that detection and estimation of a particular tap will be significantly affected by the main lobe and sidelobes from the ambiguity functions of the remaining taps. This motivates a successive cancellation approach whereby the signal contribution in \mathbf{Y} induced by a multipath tap is removed after it is detected, thus allowing subsequent taps to be detected and estimated. Successive cancellation algorithms have found widespread use in a number of communication scenarios requiring the recovery of multiple superimposed signals. In particular, interference cancellation (successive and parallel forms) is the basis of practical low-complexity multi-user decoding algorithms, which attain close to single-user bit error rate performance [38]. In our case, the superimposed signals are not signals from multiple users, but time/frequency shifted versions of the same signal. However the same principle can still be applied, and as we will see later, achieves performance close to the CRLB of a single tap channel (provided the taps are sufficiently separated in either delay or Doppler). In this direction, the first algorithm we propose is based on successive cancellation and is employed to find an initial estimate of the delay, Doppler and complex gain of each tap. The second algorithm we propose is based on parallel cancellation and is employed to refine the initial estimates. Integral to both of these algorithms is a search for the largest absolute value of a 2-D periodogram [37], and we propose a low-complexity 2-D bisection algorithm for doing this. A detailed description of each of these algorithms is given as follows.

A. Initial Estimation

Algorithm 1 describes our proposed initial successive cancellation procedure. First we initialise the residual error matrix $\mathbf{E}^{(1)}$ equal to the received noisy OFDM symbols \mathbf{Y} . At iteration $p = 1, 2, \dots, P$: we find $\hat{\tau}_p$ and $\hat{\nu}_p$ that correspond to the maximum absolute value squared of

the 2-D periodogram of $\mathbf{E}^{(p)}$; construct the $p \times p$ matrix

$$\mathbf{R}^{(p)} = \begin{pmatrix} R_{11} & R_{12} & \dots & R_{1p} \\ \vdots & \ddots & & \\ R_{p1} & R_{p2} & \dots & R_{pp} \end{pmatrix}$$

and length p vector $\mathbf{w}^{(p)} = (w_1, w_2, \dots, w_p)$ substituting the delay and Doppler estimates $\hat{\boldsymbol{\tau}}^{(p)} = (\hat{\tau}_1, \dots, \hat{\tau}_p)$ and $\hat{\boldsymbol{\nu}}^{(p)} = (\hat{\nu}_1, \dots, \hat{\nu}_p)$ into (22) and (23); re-estimate the length p complex gain vector $\hat{\mathbf{a}}^{(p)} = (\hat{a}_1, \dots, \hat{a}_p) = (\mathbf{R}^{(p)})^{-1}\mathbf{w}^{(p)}$; and finally subtract the signal contributions of all p estimated multipath components from \mathbf{Y} , which becomes the residual error matrix for the next iteration.

Typically Algorithm 1 will estimate the multipath starting from the strongest to the weakest tap, i.e. $|\hat{a}_1| > |\hat{a}_2| > \dots > |\hat{a}_P|$. Thus, for the case when P is unknown, an obvious exit criterion is to stop once $|\hat{a}_p| < \gamma$, where γ is a threshold that determines the minimum tap energy. Alternatively, the Algorithm can be modified to incorporate a model order selection rule [29].

Note that two simple modifications can be made to Algorithm 1 to further reduce complexity. Firstly, in the main loop, rather than subtracting all multipath contributions of the previously estimated components from the original signal \mathbf{Y} to obtain the residual error $\mathbf{E}^{(p)}$, simply subtract the contribution of the current estimate from the residual error of the previous iteration $\mathbf{E}^{(p-1)}$, i.e. line 6 can be replaced with $\mathbf{E}^{(p)} = \mathbf{E}^{(p-1)} - \left[\hat{a}_p^{(p)} \boldsymbol{\psi}(\hat{\nu}_p) \boldsymbol{\phi}^\dagger(\hat{\tau}_p) \right] \odot \mathbf{X}$. Secondly, rather than operating on \mathbf{Y} , one could apply the algorithm on the zero-forcing estimate of \mathbf{H} , i.e. $\hat{H}_{l,k} = Y_{l,k} X_{l,k}^* / |X_{l,k}|$. Thus, in Algorithm 1, one simply replaces \mathbf{Y} with $\hat{\mathbf{H}}$ and the Hadamard product with \mathbf{X} in lines 3 and 6 is no longer required. To summarize, we can make the following complexity-reducing modifications to Algorithm 1. Line 1: $\mathbf{E}^{(1)} = \hat{\mathbf{H}}$, Line 3: $(\hat{\tau}_p, \hat{\nu}_p) = \arg \max_{\tau, \nu} \left| \boldsymbol{\psi}^\dagger(\nu) \mathbf{E}^{(p)} \boldsymbol{\phi}(\tau) \right|^2$, and Line 6: $\mathbf{E}^{(p+1)} = \hat{\mathbf{H}} - \left[\boldsymbol{\Psi}(\hat{\boldsymbol{\nu}}^{(p)}) \text{diag}(\hat{\mathbf{a}}^{(p)}) \boldsymbol{\Phi}^\dagger(\hat{\boldsymbol{\tau}}^{(p)}) \right]$

B. Estimation Refinement

It is quite reasonable to rely solely on Algorithm 1 to estimate the delay/Doppler. Indeed similar approaches have been employed in [14, 15, 28], but without any detailed comparison to theoretical bounds. We find that the performance of Algorithm 1 is hampered by interference from undetected taps, which as we will see later, introduces a floor in the root mean squared (RMS)

error performance. Therefore we propose a refinement process based on parallel cancellation whereby for each iteration, all multipath components are removed except for the component of interest, that is subsequently re-estimated. This refinement procedure is described in detail in Algorithm 2, where $\hat{\boldsymbol{\tau}}^{(i)} = (\hat{\tau}_1^{(i)}, \dots, \hat{\tau}_P^{(i)})$, $\hat{\boldsymbol{\nu}}^{(i)} = (\hat{\nu}_1^{(i)}, \dots, \hat{\nu}_P^{(i)})$ and $\hat{\boldsymbol{a}}^{(i)} = (\hat{a}_1^{(i)}, \dots, \hat{a}_P^{(i)})$ denote the refined estimates after the i 'th iteration, and $\hat{\boldsymbol{\tau}}^{(0)} = \hat{\boldsymbol{\tau}}$, $\hat{\boldsymbol{\nu}}^{(0)} = \hat{\boldsymbol{\nu}}$ and $\hat{\boldsymbol{a}}^{(0)} = \hat{\boldsymbol{a}}$ are the initial estimates obtained from Algorithm 1. In addition, we let $\hat{\tau}_{\bar{p}}^{(i)}$, $\hat{\nu}_{\bar{p}}^{(i)}$ and $\hat{a}_{\bar{p}}^{(i)}$ denote the refined estimates at step i with element p element omitted.

Note that rather than refining for a fixed number of iterations, Algorithm 2 can be easily be modified to incorporated an early stopping criterion, e.g. by checking the improvement in the residual error $\|\mathbf{E}\|^2$. As previously described for Algorithm 1, one could apply Algorithm 2 to the zero-forcing estimate of $\hat{\mathbf{H}}$, i.e. replace \mathbf{Y} with $\hat{\mathbf{H}}$ and removing the Hadamard product with \mathbf{X} in lines 4 and 5.

C. 2-D Bisection Algorithm

As mentioned earlier, the maximisation step in line 3 Algorithm 1 and line 5 of Algorithm 2 can be solved by finding the maximum absolute value of the 2-D periodogram [37]. To perform this operation, we propose a 2-D bisection approach described as follows. First we assume $\tau_p \in (\tau_{\min}, \tau_{\max})$ and $\nu_p \in (\nu_{\min}, \nu_{\max})$ for all $p = 1, \dots, P$, i.e. the delay/Doppler of each tap is constrained to lie within predefined intervals. Let $(\tau_{\min}^{(i)}, \tau_{\max}^{(i)})$ and $(\nu_{\min}^{(i)}, \nu_{\max}^{(i)})$ denote the search interval at iteration i , and $\tilde{\boldsymbol{\tau}}^{(i)}$ and $\tilde{\boldsymbol{\nu}}^{(i)}$ denote linearly spaced vectors within these intervals, i.e.

$$\tilde{\tau}_m^{(i)} = \tau_{\min}^{(i)} + (m - 1)\Delta\tau^{(i)} \quad \tilde{\nu}_n^{(i)} = \nu_{\min}^{(i)} + (n - 1)\Delta\nu^{(i)}, \quad (27)$$

for $m = 1, \dots, M$ and $n = 1, \dots, N$, where $\Delta\tau^{(i)} = (\tau_{\max}^{(i)} - \tau_{\min}^{(i)})/M$ and $\Delta\nu^{(i)} = (\nu_{\max}^{(i)} - \nu_{\min}^{(i)})/N$ denote the bin spacing at the i 'th iteration. For each iteration of the bisection algorithm, we find the indices corresponding to the largest peak of $\boldsymbol{\Psi}^\dagger(\tilde{\boldsymbol{\nu}}^{(i)})[\mathbf{Y} \odot \mathbf{X}^*]\boldsymbol{\Phi}(\tilde{\boldsymbol{\tau}}^{(i)})$. For the next iteration, the search interval is then bisected or reduced to a smaller 2-D region, i.e. $(2\beta\Delta\tau^{(i)}, 2\beta\Delta\nu^{(i)})$, centered at the previous delay/Doppler indices (typically $\beta \geq 1/2$). A detailed description of the procedure is given in Algorithm 3. Note that for ease of exposition, the bisection process completes after a fixed number of iterations N_{bisect} . The algorithm can easily be modified to employ an early stopping criterion, e.g. exit the main loop when $\Delta\tau^{(i)} < \epsilon_\tau$ and $\Delta\nu^{(i)} < \epsilon_\nu$ to ensure a certain level of delay/Doppler resolution.

V. PERFORMANCE EVALUATION

Performance evaluation is complicated by the fact there are infinitely many possible multipath channel realisations and many OFDM system design configurations all of which can have a significant effect on the estimator's performance. To reduce our analysis, we focus on OFDM systems with similar specifications to the IEEE802.11p standard (as described in Section III). In addition, we concentrate on multipath channels typical of outdoor mobile vehicular environments [39], i.e. delay spreads not exceeding 200 nsec and Doppler differentials not exceeding 1000 Hz. For example, at a carrier frequency of 5.9 GHz, this corresponds to a maximum excess delay of 60 m and velocity differentials of 51 m/s or 183 km/hr.

Ultimately, we would like to investigate the estimator's performance for as many different multipath channel configurations as possible. However, we find that the performance is significantly affected by the location of the multipath taps in the 2-D delay/Doppler space. When two or more taps are too close to each other there is a high probability Algorithm 1 will detect these as a single tap.¹ The minimum separation distance is essentially the delay/Doppler resolution of the estimator, which is dependent on the main lobe of the ambiguity function, which in turn, is dependent on the subcarrier spacing and duration of the OFDM packet (as evidenced in (17)). When the components are sufficiently separated, the estimator's performance is dominated by AWGN and hence the CRLB (26).

To separate the above mentioned effects, we conducted Monte Carlo simulations whereby for each trial a random set of multipath taps is generated. Whilst these taps are drawn randomly, they are not i.i.d., and instead are drawn to ensure a minimum separation in delay and Doppler. This is achieved by continually drawing a vector of P delays from an i.i.d. uniform distribution on the interval $(\tau_{\min}, \tau_{\max})$ until the minimum pairwise distance between the delays is greater than a specified $\Delta\tau$. The delays are then sorted in ascending order. The Doppler offsets are generated in a similar fashion on the interval (ν_{\min}, ν_{\max}) , but with no sorting. Note that $\Delta\tau \leq (\tau_{\max} - \tau_{\min})/P$ and similarly $\Delta\nu \leq (\nu_{\max} - \nu_{\min})/P$. Whilst we fix the power delay profile, for each trial, the phase of each tap is generated randomly according to a uniform distribution over the interval $(0, 2\pi)$. Once the multipath taps are generated, the frequency domain channel coefficients are

¹In a physical sense, if these closely spaced taps are the result of first order reflections it may imply they are reflections from the same object.

generated using (8) and the received noisy symbols are generated using (7), where, without loss of generality, we assume $X_{l,k} = 1$. It is important to note how the error statistics were calculated. For each trial, RMS error statistics were only collected when all taps are detected, i.e. each tap is closest (in Euclidean distance) to a single estimate. Events when this does not occur are counted as missed detections, but are not included in the RMS error statistics. This allows us to separate error events caused by miss detections due to the transmit ambiguity function.

In our simulations we considered a $P = 3$ tap multipath channel, with power delay profile $|a_1|^2 = 0$, $|a_2|^2 = -10$ and $|a_3|^2 = -20$ dB, $(\tau_{\min}, \tau_{\max}) = (0, 200)$ nsec, $(\nu_{\min}, \nu_{\max}) = (-500, 500)$, minimum delay separation of $\Delta\tau = 66.67$ nsec and minimum Doppler separation of $\Delta\nu = 333.33$ Hz. Error statistics were collected from 10^4 trials.

Fig. 2 shows the miss detection probability for $L = 128, 256$ and 512 OFDM packet lengths. We see that when $L = 128$, the miss detection probability is greater than 10 percent. As L increases the main lobe of the ambiguity function shrinks in the Doppler domain improving the resolution of the estimator and hence reduces the miss detection probability. When $L = 512$, no miss detections were recorded for an SNR greater than 5 dB.

Fig. 3 shows the RMS estimation error results (recalling that this is restricted to instances where missed detection does not occur). The square marked curves show the RMS error when no refinement is performed, i.e. only Algorithm 1 is employed. In this case a floor in the RMS error performance is observed (caused by undetected multipath components in the successive cancellation process). When refinement is employed, as shown by the circle marked curves, the error floor is significantly reduced. Moreover, as L increases the floor does not occur until very high SNRs and the RMS error performance is primarily dominated by the CRLB (26), which is shown by the dashed curves. Thus with sufficiently long packet length, Algorithms 1 and 2 deliver single-tap performance, i.e. are able to accurately cancel the contributions of “interfering” taps.

It is interesting to translate the estimator performance into range/velocity resolution. Considering $L = 512$ and SNR 20 dB, the 3-standard-deviation values for the -20 dB tap are 9 ns and 15 Hz. This corresponds to range resolution of 2.7 m and relative velocity resolution (at 5.9GHz) of 0.77 m/s (2.7 km/h). This clearly demonstrates the capability to accurately resolve quite challenging multipath channels.

VI. CONCLUSION

In this paper we examined amplitude, delay and Doppler estimation of the multipath channel taps from OFDM signal transmission in a doubly selective mobile environment. Under certain practical system design and mobile channel assumptions, we showed that the frequency domain channel coefficients for an entire OFDM packet can be written as the superimposition of 2-D complex sinusoids. The angular frequency of each sinusoid is proportional to the delay and Doppler of a particular multipath tap.

ML estimation of the delay/Doppler requires non-linear least squares minimisation, which is computationally infeasible for practical implementation. We therefore proposed a low complexity suboptimal estimation method, based on successive cancellation, whereby multipath components are removed once they are detected. The complexity reduction results from a simplification of the channel model, where time variations manifest only as Doppler frequency offsets for each tap. For a single tap channel, this method is maximum likelihood. The performance of this successive cancellation approach can be degraded by interference from taps that are yet to be detected in future iterations. To remedy this, we proposed a refinement algorithm based on parallel cancellation, i.e. all estimated multipath components are subtracted except the component of interest, which is subsequently re-estimated.

The performance of our estimator was shown to be dominated by two effects: separation of the multipath taps in the delay/Doppler plane; and noise. When two or more taps are close together in the 2-D delay/Doppler space, the estimator may detect these as single tap, resulting in missed detections and significantly degrading the RMS error of other detected taps. When the multipath taps are sufficiently separated in delay/Doppler the estimator performance is dominated by noise and hence the RMS error of the refined estimates are very close the CRLB of a single 2-D sinusoid in additive white Gaussian noise. We believe the missed detections are caused by the transmit ambiguity function: broadness of the main lobe affects the delay/Doppler resolution; and sidelobes of components that have not been sufficiently subtracted can mask weaker taps. However, a detailed analytic investigation of these effects is beyond the scope of this paper and the subject of future work.

Note that although our results assume delay spreads less than the cyclic prefix, our proposed estimator still works well without this restriction. Multipath taps with delay exceeding the cyclic

prefix will introduce inter-symbol interference. The estimator views this interference as extra noise on the received symbols. Thus, as long as AWGN dominates, this extra interference will have negligible effect on performance.

APPENDIX I

DERIVATION OF RECEIVER MATCHED FILTER OUTPUT

For clarity we repeat the transmitted signal,

$$x(t) = \sum_{l'} x_{l'}(t) = \frac{1}{\sqrt{KL}} \sum_{l',k'} X_{l',k'} w(t - (l' - 1)T_d) e^{j2\pi(k'-1 - \lfloor K/2 \rfloor)(t - T_{cp})/T}. \quad (28)$$

Application of the channel response (4) to the transmitted signal (28) yields

$$\begin{aligned} y(t) &= x(t) * h(t, \tau) + z(t) = \int_{-\infty}^{\infty} x(t - \tau) h(t, \tau) d\tau \\ &= \frac{1}{\sqrt{KL}} \sum_{l',k',p} a_p X_{l',k'} \int_{-\infty}^{\infty} g(\tau - \tau_p) w(t - \tau - (l' - 1)T_d) e^{-2\pi\nu_p t} e^{j2\pi(k'-1 - \lfloor K/2 \rfloor)(t - \tau - T_{cp})/T} d\tau + z(t) \\ &= \frac{1}{\sqrt{KL}} \sum_{l',k',p} a_p X_{l',k'} e^{-j2\pi(k'-1 - \lfloor K/2 \rfloor)T_{cp}/T} e^{-j2\pi(\nu_p - \frac{k'-1}{T} + \frac{K}{2T})t} s_{l',k'}(t, \tau_p) + z(t), \end{aligned} \quad (29)$$

where the integral

$$s_{l',k'}(t, \tau_p) = \int_{-\infty}^{\infty} g(\tau - \tau_p) e^{-j2\pi(k'-1 - \lfloor K/2 \rfloor)\tau/T} w(t - \tau - (l' - 1)T_d) d\tau, \quad (30)$$

is simply the convolution of a time/frequency translated filter response $g(t)$ and time shifted window function $w(t)$. Using the appropriate properties of Fourier transforms, the Fourier transform of (30) can be written as

$$S_{l',k'}(f, \tau_p) = e^{-j2\pi\tau_p \left[\frac{k'-1}{T} - \frac{K}{2T} + f \right]} e^{-j2\pi f(l'-1)T_d} G \left(f + \frac{k'-1}{T} - \frac{K}{2T} \right) W(f), \quad (31)$$

where $G(f)$ and $W(f)$ denote the Fourier transforms of $g(t)$ and $w(t)$ respectively. In practical OFDM systems the passband bandwidth of $G(f)$ is typically greater than K/T and the bandwidth of $W(f)$ is typically less than $1/T$, e.g. for the simple case $\tilde{w}(t) = \frac{1}{\sqrt{T_d}}$, then $W(f) = \sqrt{T_d} e^{-j\pi f T_d} \text{sinc}(\pi f T_d)$. Moreover, in many OFDM standards the outer subcarriers are null subcarriers. Hence assuming negligible passband ripple then $G \left(f + \frac{k'-1}{T} - \frac{K}{2T} \right) \approx 1$ for $k' = 1, \dots, K$ and $|f| < 1/(2T)$. Therefore,

$$S_{l',k'}(f, \tau_p) \approx e^{-j2\pi\tau_p \left[\frac{k'-1}{T} - \frac{K}{2T} + f \right]} e^{-j2\pi f(l'-1)T_d} W(f). \quad (32)$$

Thus, taking the inverse Fourier transform yields

$$\begin{aligned} s_{l',k'}(t, \tau_p) &\approx e^{-j2\pi\tau_p\left[\frac{k'-1}{T}-\frac{K}{2T}\right]} \int_{-\infty}^{\infty} W(f)e^{j2\pi f[t-\tau_p-(l'-1)T_d]} df \\ &= e^{-j2\pi\tau_p\left[\frac{k'-1}{T}-\frac{K}{2T}\right]} w(t - \tau_p - (l' - 1)T_d). \end{aligned} \quad (33)$$

Substituting (33) into (29) gives,

$$\begin{aligned} y(t) &= \frac{1}{\sqrt{KL}} \sum_{l',k',p} a_p X_{l',k'} e^{-j2\pi(k'-1-\lfloor K/2 \rfloor)T_{cp}/T} e^{-j2\pi\left(\nu_p - \frac{k'-1}{T} + \frac{K}{2T}\right)t} \\ &\quad \times e^{-j2\pi\tau_p\left(\frac{k'-1}{T} - \frac{K}{2T}\right)} w(t - \tau_p - (l' - 1)T_d) + z(t), \end{aligned} \quad (34)$$

The receiver now performs the matched filter to the transmitted sinusoids (less the cyclic prefix), i.e.

$$\begin{aligned} Y_{l,k} &= \frac{1}{\sqrt{KL}} \int_{T_{cp}+(l-1)T_d}^{lT_d} y(t)w^*(t - lT_d)e^{-j2\pi(k-1-\lfloor K/2 \rfloor)(t-T_{cp})/T} dt \\ &= \frac{1}{KL} \sum_{l',k',p} a_p X_{l',k'} e^{-j2\pi\tau_p\left(\frac{k'-1}{T} - \frac{K}{2T}\right)} e^{-j2\pi(k'-k)T_{cp}/T} \\ &\quad \times \int_{T_{cp}+(l-1)T_d}^{lT_d} w(t - \tau_p - (l' - 1)T_d)w^*(t - (l - 1)T_d)e^{-j2\pi\left(\nu_p + \frac{k-k'}{T}\right)t} dt + Z_{l,k} \\ &= \frac{1}{KL} \sum_{l',k',p} a_p X_{l',k'} e^{-j2\pi\tau_p\left(\frac{k'-1}{T} - \frac{K}{2T}\right)} e^{-j2\pi(k'-k)T_{cp}/T} e^{-j2\pi\left(\nu_p + \frac{k-k'}{T}\right)(l-1)T_d} \\ &\quad \times \hat{A}_w\left(\tau_p + (l' - l)T_d, \nu_p + \frac{k - k'}{T}\right) + Z_{l,k}, \end{aligned} \quad (35)$$

where

$$\hat{A}_w(\tau, \nu) = \int_{T_{cp}}^{T_d} w(t - \tau)w^*(t)e^{-j2\pi\nu t} dt, \quad (36)$$

which resembles the ambiguity function of $w(t)$.² In practical OFDM systems, usually $\max_p \tau_p < T_{cp}$ and $\max_p \nu_p \ll 1/T$ and the windowing function is usually designed such that $\hat{A}_w\left(\tau_p + (l' - l)T_d, \nu_p + \frac{k-k'}{T}\right) \approx 0$ for $k \neq k'$ or $l \neq l'$. Hence we may write,

$$\begin{aligned} Y_{l,k} &= \frac{1}{KL} \sum_p a_p X_{l,k} e^{-j2\pi\tau_p\left(\frac{k-1}{T} - \frac{K}{2T}\right)} e^{-j2\pi\nu_p T_d(l-1)} \hat{A}_w(\tau_p, \nu_p) + Z_{l,k} \\ &= \frac{1}{KL} \sum_p \tilde{a}_p X_{l,k} e^{-j2\pi(k-1)\tau_p/T} e^{-j2\pi(l-1)\nu_p T_d} + Z_{l,k}, \end{aligned} \quad (37)$$

²The function $\hat{A}_w(\tau, \nu)$ is not quite the ambiguity function of $w(t)$ because of the limits of integration.

where $\tilde{a}_p = e^{-j\pi K\tau_p/T} \hat{A}_w(\tau_p, \nu_p)$. With some slight abuse of notation, for the remainder of the paper for brevity of notation (and without loss of generality) we will replace \tilde{a}_p with a_p . Defining $H_{l,k}$ according to (8), we obtain (7).

REFERENCES

- [1] J. G. Proakis, *Digital Communications*, McGraw-Hill, 4 edition, 2000.
- [2] A. Goldsmith, *Wireless Communications*, Cambridge University Press, 2005.
- [3] A. Peled and A. Ruiz, "Frequency domain data transmission using reduced computational complexity algorithms," in *Int. Conf. on Acoustics, Speech, and Sig. Proc.*, Apr 1980, vol. 5, pp. 964–967.
- [4] L. Cimini, "Analysis and simulation of a digital mobile channel using orthogonal frequency division multiplexing," *IEEE Trans. Commun.*, vol. 33, no. 7, pp. 665–675, Jul. 1985.
- [5] R. van Nee and R. Prasad, *OFDM for Wireless Multimedia Communications*, Artech House Publishers, 1999.
- [6] R. van Nee, V. K. Jones, G. Awater, A. van Zelst, J. Gardner, and G. Steele, "The 802.11n MIMO-OFDM standard for wireless LAN and beyond," *Wireless Personal Commun.*, vol. 37, pp. 445–453, 2006.
- [7] G. Hiertz, D. Denteneer, L. Stibor, Y. Zang, X.P. Costa, and B. Walke, "The IEEE 802.11 universe," *IEEE Commun. Mag.*, vol. 48, no. 1, pp. 62–70, Jan. 2010.
- [8] "802.11p-2010 IEEE standard for information technology – Telecommunications and information exchange between systems – Local and metropolitan area networks – Specific requirements part 11: Wireless LAN medium access control (MAC) and physical layer (PHY) spec," 2010.
- [9] D. Haley P. Alexander and A. Grant, "Cooperative intelligent transport systems: 5.9 GHz field trials," *Submitted to Proc. IEEE*, 2010.
- [10] W. Kozek and A. F. Molisch, "Nonorthogonal pulseshapes for multicarrier communications in doubly dispersive channels," *IEEE J. Sel. Areas Commun.*, vol. 16, no. 8, pp. 1579–1589, Oct. 1998.
- [11] K. Liu, T. Kadous, and A. M. Sayeed, "Orthogonal time-frequency signaling over doubly dispersive channels," *IEEE Trans. Inform. Theory*, vol. 50, no. 11, pp. 2583–2603, Nov 2004.
- [12] G. Tauböck and F. Hlawatsch, "On the capacity-achieving input covariance for multicarrier communications over doubly selective channels," in *IEEE Int. Symp. Inform. Theory*, 2007.
- [13] J. Karedal, F. Tufvesson, N. Czink, A. Paier, C. Dumard, T. Zemen, C. Mecklenbrauker, and A. Molisch, "A geometry-based stochastic MIMO model for vehicle-to-vehicle communications," *IEEE Trans. Wireless Commun.*, vol. 8, no. 7, pp. 3646–3657, Jul 2009.
- [14] T. A. Thomas, T. P. Krauss, and F. W. Vook, "CHAMPS: A near-ML joint Doppler frequency/ToA search for channel characterization," in *IEEE Vehic. Technol. Conf.*, 6-9 Oct. 2003, pp. 74–78.
- [15] C. R. Berger, S. Zhou, and P. Willett, "Signal extraction using compressed sensing for passive radar with OFDM signals," in *11th International Conference on Information Fusion*, Jan 2008, pp. 1–6.
- [16] M. Cherniakov and D. V. Nezlin, *Bistatic radar: principles and practice*, John Wiley, Chichester, 2007.
- [17] E. J. Candès and M. B. Wakin, "An introduction to compressive sampling," *IEEE Signal Processing Magazine*, vol. 21, no. 2, Mar 2008.
- [18] D. Needell and R. Vershynin, "Uniform uncertainty principle and signal recovery via regularized orthogonal matching pursuit," <http://arxiv.org/pdf/0707.4203v4>, Mar 2008.

- [19] D. Needell, J. Tropp, and R. Vershynin, "Greedy signal recovery review," in *Asilomar Conf. on Signals Systems and Computers*, Oct. 2008, pp. 1048–1050.
- [20] G. Tauböck and F. Hlawatsch, "A compressed sensing technique for ofdm channel estimation in mobile environments: exploiting channel sparsity for reducing pilots," in *IEEE Int. Conf. on Acoustics Speech and Signal Proc.*, 2008.
- [21] G. Tauböck, F. Hlawatsch, D. Eiwien, and H. Rauhut, "Compressive estimation of doubly selective channels in multicarrier systems: Leakage effects and sparsity-enhancing processing," *IEEE J. Sel. Topics in Sig. Proc.*, vol. 4, no. 2, pp. 255–271, Apr. 2010.
- [22] I. C. Wong and B. L. Evans, "Sinusoidal modeling and adaptive channel prediction in mobile OFDM systems," *IEEE Trans. Sig. Proc.*, vol. 56, no. 4, pp. 1601–1615, Apr. 2008.
- [23] I. C. Wong and B. L. Evans, "Joint channel estimation and prediction OFDM systems," in *IEEE GLOBECOM*, St. Louis, MO, Dec. 2005, p. 2259.
- [24] H. Chien, *2-D estimation from AR models*, Ph.D. thesis, Univ. of Rhode Island, Kingston, RI, May 1981.
- [25] S. Kay and R. Nekovei, "An efficient two-dimensional frequency estimator," *IEEE Trans. Acoustics, Speech and Sig. Proc.*, vol. 38, no. 10, pp. 1807–1810, Oct 1990.
- [26] Y. Bresler and A. Macovski, "Exact maximum likelihood parameter estimation of superimposed exponential signals in noise," *IEEE Trans. Acoustics, Speech and Sig. Proc.*, vol. 34, no. 5, pp. 1081–1089, Oct. 1986.
- [27] C. Rao, L. Zhao, and B. Zhou, "Maximum likelihood estimation of 2-D superimposed exponential signals," *IEEE Trans. Sig. Proc.*, vol. 42, no. 7, pp. 1795–1802, July 1994.
- [28] M. Kliger and J. M. Francos, "MAP model order selection rule for 2-D sinusoids in white noise," *IEEE Trans. Sig. Proc.*, vol. 53, no. 7, pp. 2563–2575, July 2005.
- [29] P. Stoica and Y. Selén, "Model-order selection: a review of information criterion rules," *IEEE Sig. Proc. Mag.*, pp. 36–47, 2004.
- [30] V. Pereyra, "Iterative methods for solving nonlinear least squares problems," *SIAM J. Numer. Anal.*, vol. 4, no. 1, pp. 27–36, Mar. 1967.
- [31] S. Boyd and L. Vandenberghe, *Convex Optimization*, Cambridge University Press, 2004.
- [32] M. Skolnik, *Introduction to Radar Systems*, McGraw-Hill, New York, 3rd edition, 2002.
- [33] R. Horn and C. R. Johnson, *Matrix Analysis*, Cambridge University Press, 1985.
- [34] IEEE 802.11a-1999, "Supplement to IEEE Standard for Information Technology - Telecommunications and Information Exchange Between Systems - Local and Metropolitan Area Networks - Specific Requirements. Part 11: Wireless LAN Medium Access Control (MAC) and Physical Layer (PHY) Specifications: High-Speed Physical Layer in the 5 GHz Band," 1999.
- [35] B. O'Hara and A. Petrick, *The IEEE 802.11 Handbook: A Designer's Companion*, IEEE Press, 1999.
- [36] G. H. Golub and V. Pereyra, "The differentiation of pseudo-inverses and non-linear least squares problems whose variables separate," *SIAM J. Numer. Anal.*, vol. 10, no. 2, pp. 413–432, Apr. 1973.
- [37] S. M. Kay, *Modern spectral estimation: theory and application*, Prentice Hall, Englewood Cliffs, N.J., 1988.
- [38] C. Schlegel and A. Grant, *Coordinated Multiuser Communications*, Springer, 2006.
- [39] P. Alexander, D. Haley, and A. Grant, "Outdoor mobile broadband access with 802.11," *IEEE Commun. Mag.*, vol. 45, no. 11, pp. 108–114, Nov. 2007.

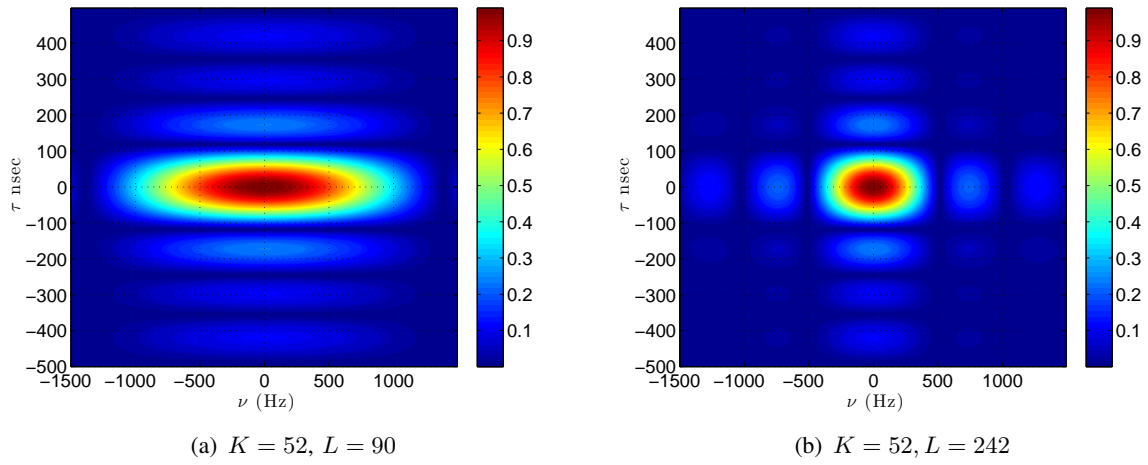


Fig. 1. Magnitude contour plot of the ambiguity function (18) of an 802.11a OFDM system with PSK modulation, $T = 6.4 \mu\text{sec}$, $T_d = 8 \mu\text{sec}$

Algorithm 1: Initial estimation via successive cancellation.

- 1: $\mathbf{E}^{(1)} = \mathbf{Y}$
 - 2: **for** $p = 1, \dots, P$ **do**
 - 3: $(\hat{\tau}_p, \hat{\nu}_p) = \arg \max_{\tau, \nu} \left| \boldsymbol{\psi}^\dagger(\nu) \left(\mathbf{E}^{(p)} \odot \mathbf{X}^* \right) \boldsymbol{\phi}(\tau) \right|^2$
 - 4: Construct $\mathbf{R}^{(p)}$ and $\mathbf{w}^{(p)}$ using (22) and (23) with $\hat{\tau}_1, \dots, \hat{\tau}_p$ and $\hat{\nu}_1, \dots, \hat{\nu}_p$.
 - 5: $\hat{\mathbf{a}}^{(p)} = (\mathbf{R}^{(p)})^{-1} \mathbf{w}^{(p)}$
 - 6: $\mathbf{E}^{(p+1)} = \mathbf{Y} - \left[\boldsymbol{\Psi}(\hat{\boldsymbol{\nu}}^{(p)}) \text{diag}(\hat{\mathbf{a}}^{(p)}) \boldsymbol{\Phi}^\dagger(\hat{\boldsymbol{\tau}}^{(p)}) \right] \odot \mathbf{X}$
 - 7: **end for**
-

Algorithm 2: Estimate refinement algorithm.

- 1: $\hat{\boldsymbol{\tau}}^{(0)} = \hat{\boldsymbol{\tau}}, \hat{\boldsymbol{\nu}}^{(0)} = \hat{\boldsymbol{\nu}}$ and $\hat{\boldsymbol{a}}^{(0)} = \hat{\boldsymbol{a}}$
 - 2: **for** $i = 1, \dots, N$ **do**
 - 3: **for** $p = 1, \dots, P$ **do**
 - 4: $\mathbf{E} = \mathbf{Y} - \left[\boldsymbol{\Psi}(\hat{\boldsymbol{\nu}}_p^{(i-1)}) \text{diag}(\hat{\boldsymbol{a}}_p^{(i-1)}) \boldsymbol{\Phi}^\dagger(\hat{\boldsymbol{\tau}}_p^{(i-1)}) \right] \odot \mathbf{X}$
 - 5: $(\hat{\tau}_q^{(i)}, \hat{\nu}_q^{(i)}) = \arg \max_{\tau, \nu} |\boldsymbol{\psi}^\dagger(\nu) (\mathbf{E} \odot \mathbf{X}^*) \boldsymbol{\phi}(\tau)|^2$
 - 6: **end for**
 - 7: $\hat{\boldsymbol{a}}^{(i)} = \mathbf{R}^{-1}(\hat{\boldsymbol{\tau}}^{(i)}, \hat{\boldsymbol{\nu}}^{(i)}) \mathbf{w}(\hat{\boldsymbol{\tau}}^{(i)}, \hat{\boldsymbol{\nu}}^{(i)})$
 - 8: **end for**
-

Algorithm 3: 2-D Bisection Algorithm.

- 1: Initialise $(\tau_{\min}^{(0)}, \tau_{\max}^{(0)}) = (\tau_{\min}, \tau_{\max})$ and $(\nu_{\min}^{(0)}, \nu_{\max}^{(0)}) = (\nu_{\min}, \nu_{\max})$.
 - 2: **for** $i = 1, \dots, N_{\text{bisect}}$ **do**
 - 3: $\Delta\tau^{(i)} = (\tau_{\max}^{(i-1)} - \tau_{\min}^{(i-1)})/M$, $\Delta\nu^{(i)} = (\nu_{\max}^{(i-1)} - \nu_{\min}^{(i-1)})/N$
 - 4: Construct $\tilde{\tau}^{(i)}$ and $\tilde{\nu}^{(i)}$ using (27).
 - 5: $\Upsilon^{(i)} = \Psi^\dagger(\tilde{\nu}^{(i)}) [\mathbf{Y} \odot \mathbf{X}^*] \Phi(\tilde{\tau}^{(i)})$
 - 6: $(\hat{n}, \hat{m}) = \arg \max_{n,m} |\Upsilon_{n,m}^{(i)}|^2$
 - 7: $\tau_{\max}^{(i)} = \tilde{\tau}_{\hat{m}}^{(i)} + \beta\Delta\tau^{(i)}$, $\tau_{\min}^{(i)} = \tilde{\tau}_{\hat{m}}^{(i)} - \beta\Delta\tau^{(i)}$
 - 8: $\nu_{\max}^{(i)} = \tilde{\nu}_{\hat{n}}^{(i)} + \beta\Delta\nu^{(i)}$, $\nu_{\min}^{(i)} = \tilde{\nu}_{\hat{n}}^{(i)} - \beta\Delta\nu^{(i)}$
 - 9: **end for**
 - 10: $\hat{\tau} = \tilde{\tau}_{\hat{m}}^{(I)}$, $\hat{\nu} = \tilde{\nu}_{\hat{n}}^{(I)}$.
-

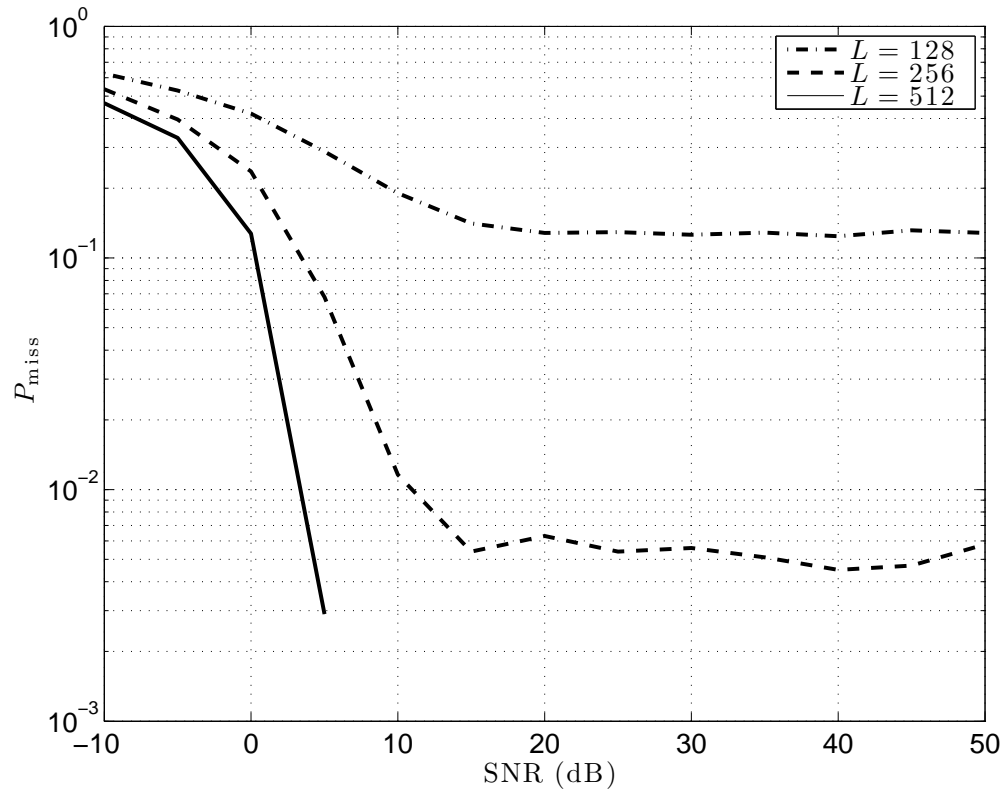
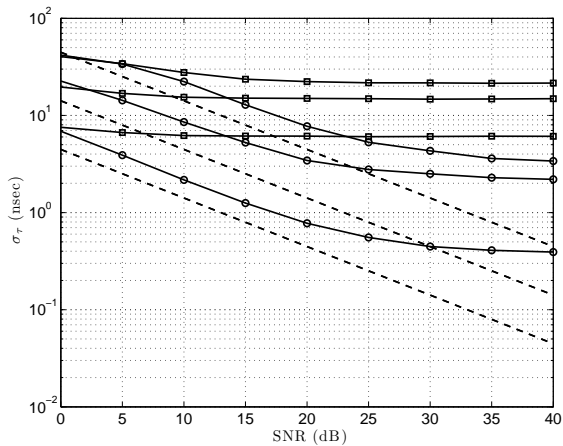
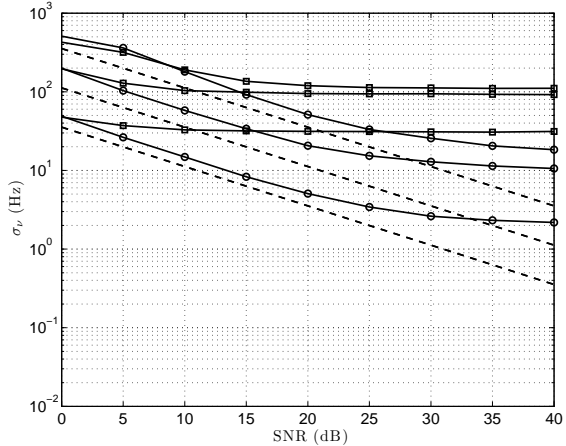


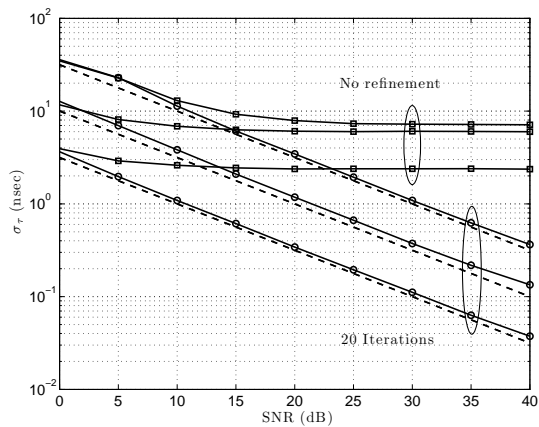
Fig. 2. Probability of miss detecting all taps of a $P = 3$ tap multipath channel.



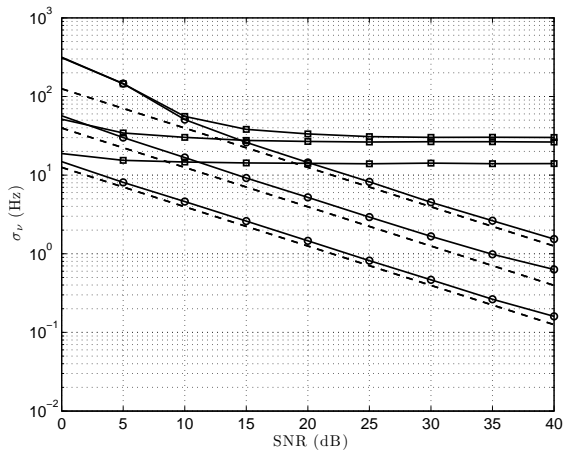
(a) $L = 128$



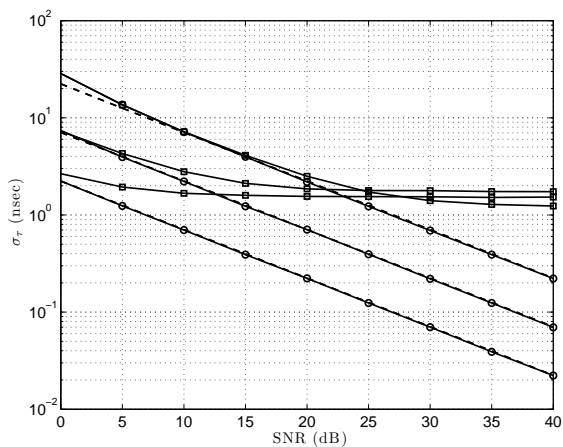
(b) $L = 128$



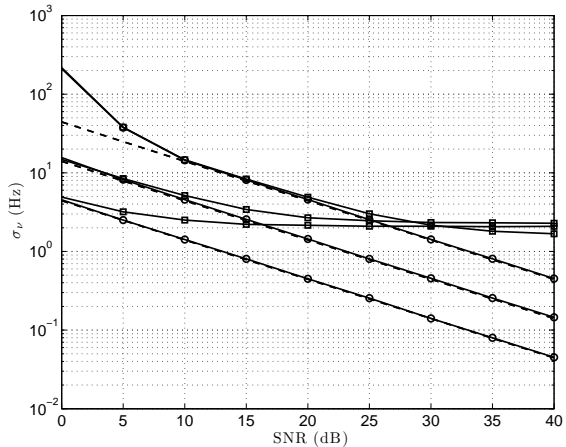
(c) $L = 256$



(d) $L = 256$



(e) $L = 512$



(f) $L = 512$

Fig. 3. Three tap estimation root-mean squared (RMS) error. Dashed lines show the CRLB (26) (single-tap estimation). Solid lines with squares show RMS error performance of Algorithm 1 only. Solid lines with circles show the RMS error performance after refinement Algorithm 2 with 20 iterations.